ACOUSTICS 2012

Quantification of freshly-excised human lymph node tissue using high-frequency ultrasound

J. Mamou[a], A. Coron[b], E. Saegusa-Beecroft[c], M. Hata[c], M. L. Oelze[d], E. Yanagihara[c], T. Yamaguchi[e], P. Laugier[b], J. Machi[c] and E. J. Feleppa[a]

[a]Lizzi Center for Biomedical Engineering, Riverside Research, 156 William St., 9th Floor, New York, 10038, USA
[b]Laboratoire d'Imagerie Paramétrique, 15 Rue de l'école de Médecine 75006 Paris
[c]Kuakini Medical Center and University of Hawaii, 405 N. Kuakini, Honolulu, 96817, USA
[d]University of Illinois at Urbana-Champaign, 405 N. Mathews, Urbana, 61801, USA
[e]CFME, Chiba University, 1-33 Yayoicho, Chiba, Japan
jmamou@riversideresearch.org

Quantitative ultrasound (QUS) methods using high-frequency transducers (i.e., > 20 MHz) permit characterization of tissue microstructure and organization using system-independent estimates. In this study, lymph nodes excised during lymphadenectomy from cancer patients were evaluated using three-dimensional (3D) high-frequency QUS methods. The long-term objective of these studies is to develop 3D QUS methods for detecting lymph-node metastases. Detection of metastases is critically important for cancer staging, treatment, and optimal patient management. A custom laboratory scanning system was used to acquire radio-frequency (RF) data in 3D from excised lymph nodes using a 26-MHz center-frequency transducer. Overlapping 1-mm cylindrical regions-of-interest (ROIs) of the RF data were processed to yield 13 QUS estimates associated with tissue microstructure. QUS estimates were obtained from 255 nodes from 162 colorectal-, gastric-, and breast-cancer patients. Cancer-detection performance was assessed for individual estimates and linear combinations of estimates. ROC results demonstrated excellent classification. For colorectal- and gastric-cancer nodes, the areas under the ROC curves (AUCs) were above 0.94. Slightly poorer results (AUC=0.87) were obtained for breast-cancer nodes. Images based on QUS parameters also permitted localization of cancer foci in some micrometastatic cases. Therefore, these advanced 3D QUS methods potentially can be valuable for detecting small clinically-significant metastatic foci in dissected lymph nodes which can be missed during routine histology procedures.

1 Introduction

Typical B-mode ultrasound images are mostly qualitative and simply display relative changes in acoustical impedance. They have spatial resolutions on the order of the wavelength and are used to describe tissue morphology. During the past three decades, several successful studies have led to theories and protocols using ultrasound to quantify tissue properties with system-independent estimates. In these studies, several different tissue properties have been investigated as tools to diagnose disease states [1], to monitor tissue response to therapies [2], or more fundamentally, to better understand the intricate relationship between ultrasound scattering and tissue properties [3, 4]. Furthermore, high-frequency ultrasound (HFU, >20 MHz) combined with quantitative ultrasound (QUS) permits quantification of tissue properties at the microscopic level with spatial resolutions below 100 μm. In this study, HFU was used to develop novel three-dimensional (3D) QUS methods to detect and localize metastatic regions in freshly-excised lymph nodes from cancer patients who were undergoing a lymphadenectomy.

However, typical HFU imaging suffers from two main limitations. First, HFU images have a limited depth-of-field because they are usually obtained using a single-element transducer with a low F-number; and second, penetration depth is limited because of the high attenuation at high frequencies. Nevertheless, several successful studies have demonstrated the unique ability of HFU systems to image shallow or low-attenuation tissues for biomedical applications requiring fine resolution. For example, recent HFU studies have shown success for small-animal [5] or ocular [6] imaging. In the present study, typical lymph nodes have sizes ranging from a few millimeters to more than 1 cm. Therefore, they remain small enough to be investigated using HFU.

Our group previously described the basis of our innovative 3D QUS methods to characterize lymph-node tissues from cancer patients [7]. These methods demonstrated a potential to determine the presence or absence of metastatic cancer in lymph nodes reliably. Accurate cancer detection is critical for staging and treating the disease. Since our initial successful QUS studies [7, 8], we have improved our methods by adding five novel QUS parameters and applying them to a larger number of lymph nodes from colorectal-, gastric- and breast-cancer patients.

In the present study, 13 QUS parameters were estimated and used for classification. Four QUS estimates were obtained by quantifying the backscattered spectra deduced from the radio-frequency (RF) echo signals [3, 7, 9] and four QUS estimates quantified the statistics of the envelope-detected echo signals. Specifically, the four envelope-statistics parameters were obtained from the Nakagami and the more-complex homodyned-K (HK) distribution [8]. Finally, the remaining five QUS estimates were also envelope-based but did not rely on a specific model; instead, they elegantly quantified the differences between the envelope statistics and Rayleigh statistics. The envelope-based QUS estimates are derived from fit parameters associated with the envelope; they hypothetically provide an additional means of distinguishing among tissue types, and they complement the spectral-based QUS estimates [10].

2 Methods

2.1 Surgery and 3D ultrasound data acquisition

Lymphadenectomy surgery was performed at the Kuakini Medical Center (KMC) in Honolulu, HI. Patients with histologically proven colorectal, stomach, or breast cancers were recruited. During surgery, several lymph nodes were excised and sent to the pathology laboratory at KMC where they were grossly prepared for histology. Individual lymph nodes were immersed in an isotonic saline (0.9% sodium chloride) bath at room temperature. Individual lymph nodes were scanned in 3D using a single-element spherically-focused transducer (PI30, Olympus NDT, Waltham, MA) having an aperture of 6.1 mm and a focal length of 12.2 mm. The transducer had a center frequency of 25.6 MHz and a -6 dB fractional bandwidth of 67%. The ultrasound RF echo signals were digitized with a sampling frequency of 400 MHz with 8-bit accuracy. Adjacent planes and RF lines were 25 μm apart to cover the entire node in 3D with sufficient spatial sampling.

2.2 Histology processing

Following 3D ultrasound scanning, each lymph node underwent non-standard histology processing: the node was inked to recover orientation, cut in half, embedded in a cassette, fixed, sectioned at 65 μm intervals, stained with H&E, and digital images of the slides were obtained with a high-quality high-throughput slide scanner (NanoZoomer, Hamamatsu, Japan) with a pixel resolution of 0.46 μm or with a

digital camera (FujiFilm FinePix S9100; Fuji Photo Film, Tokyo, Japan) equipped with Hoya 12 and 14 close-up lenses (Hoya Corp., Tokyo, Japan). Metastatic regions were then highlighted in each digital image using custom software.

Following digitization, a 3D histology volume was reconstructed from the adjacent images and co-registered with the 3D ultrasound data using the visible ink on the edges of the tissue.

2.3 QUS parameter estimation

To obtain the 13 QUS estimates, the 3D RF volume of data was separated in overlapping 3D cylindrical regions-of-interest (ROIs) of 1-mm diameter and 1-mm length. Within each ROI, the normalized spectrum was estimated and used to obtain four QUS estimates using two independent ultrasound scattering models [7]. Specifically, the spectral slope and the spectral intercept were obtained from a straight-line scattering model and the effective scatterer size and acoustic concentration were obtained from a Gaussian scattering model.

Similarly, the probability density function of the envelope of the ROI was estimated and used to obtain the remaining 9 QUS estimates by fitting two different envelope-statistics models (i.e., Nakagami and Homodyned-K) and by quantifying the difference between the PDF of the ROI and the Rayleigh PDF [8,11]. (Rayleigh statistics are expected when ultrasound speckle is fully developed.)

2.4 Classification

All the QUS estimates obtained from lymph nodes entirely filled or entirely devoid of metastatic tissue were used to train and test the classifiers. Linear-discriminant analysis was used to combine the 13 QUS estimates to maximize the distinction between cancerous and non-cancerous tissue. A step-wise approach was implemented to discard QUS estimates that did not significantly contribute to classification and to prevent overclassification. Additionally, because of their known histologic differences, lymph nodes were separated by organ for this analysis. The quality of the classifiers was assessed by using a leave-one-out procedure and computing the resulting specificity and sensitivity. Finally, classification performance was quantified by computing ROC curves and estimating the area under the ROC curve (AUC) for each organ.

3 Results

3.1 Illustrative QUS images

To illustrate the results, Figure 1 displays representative results obtained from two lymph nodes from two patients diagnosed with colon cancer. Figures 1a and 1b display an effective-scatterer-size parametric image at a fixed depth near the transducer focus and the photomicrograph of the corresponding histologic thin section. The histology revealed that this lymph node was non-metastatic. Similarly, Figs. 1c and 1d display the images for a metastatic lymph node. The pathologist indicated that this lymph node was entirely metastatic. For each lymph node, the histology and scatterer-size images are on the same scale for easier comparison, and segmentation results are shown in Figs. 1a and 1c by the green and red highlights. The green and red highlights surround the fat and lymph-node tissue, respectively. Figure 1 reveals that the histology images are slightly smaller in size than the tissue region of the ultrasound images because of tissue shrinkage during fixation. Figures 1a and 1c show great contrast in scatterer-size estimates. The same color scale was used for both images. The metastatic lymph node displays larger scatterer-size values. The average scatterer-size estimates for each entire lymph node was 21.3 ± 1.6 μm for the non-metastatic node and 38.9 ± 3.0 μm for the metastatic node. These illustrative results suggest that larger scatterer size may reliably indicate metastatic regions within lymph nodes.

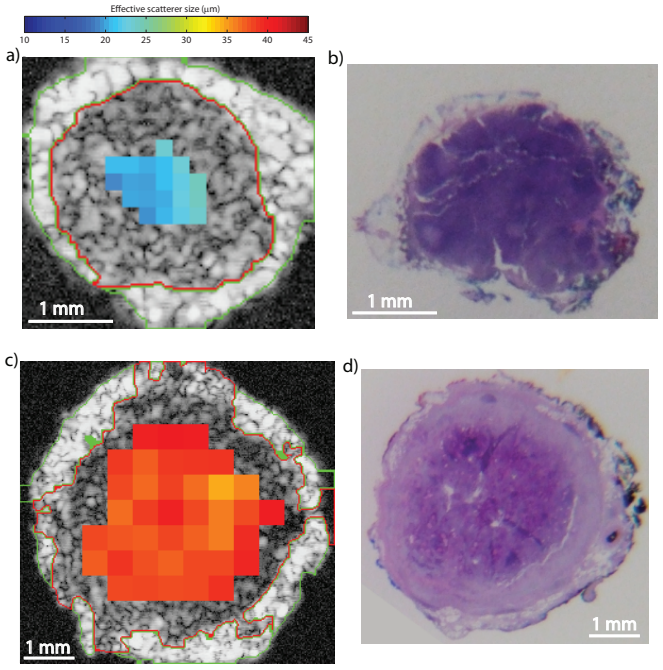

Figure 1: Illustrative results obtained with a non-metastatic lymph node (a and b) and a nearly entirely metastatic lymph node (c and d). a) and c): parametric cross-sectional images displaying effective scatterer-size estimates. b) and d) histologic thin section corresponding to a) and c), respectively. Segmentation results are shown by the green and red highlights in a) and c).

3.2 Classification performance

In total, over 250 lymph nodes from over 160 patients were entirely processed and Table 1 presents the classification performance results. The colorectal-cancer results are very satisfactory and excellent classification performance was obtained with an AUC value of 0.950. Note that the step-wise procedure rejected all but two QUS estimates to perform the classification. The gastric-cancer results are very similar and equally satisfactory, although because of the limited number of cases, greater uncertainty exists. In previous reports, the gastric-cancer nodes were analyzed with the colorectal nodes because their histologic differences are minute [8] and because the number of cases was insufficient for independent analysis. As the number of gastric-cancer cases increases, our methods will be tested for their ability at tracking these minute differences. For the gastric-cancer cases, the step-wise analysis kept four QUS estimates for optimal classification. The breast-cancer nodes are structurally very

different from the gastric- and colorectal-cancer nodes, and classification performance was slightly poorer with an AUC of 0.870, a sensitivity of 66.7% and a specificity of 86.3%. These breast-cancer results were obtained using four QUS estimates.

Table 1: Classification performance of QUS. Areas under the ROC curve (AUC) and 95% confidence interval are presented. Sensitivity and specificity were obtained using linear-discriminant analysis with a leave-one-out procedure.

Primary Organ	Patient number	Cancerous nodes	Non-cancerous nodes	ROC AUC	Sensitivity	Specificity
Colorectal	75	21	115	0.950±0.022	71.4%	91.3%
Gastric	16	5	19	0.947±0.051	100%	73.7%
Breast	71	15	80	0.870±0.048	66.7%	86.3%

3.3 Towards a tool to guide pathologists to suspicious regions

Interactive 3D visualization software was developed that permits us to dissect the lymph node virtually at three orthogonal planes in the 3D dataset. Three panels show the ultrasound data while the fourth displays the co-registered histology. Figure 2 shows a screen capture of the interactive software for a partially-metastatic breast-cancer lymph node. The red highlights in the three ultrasound cross-sections indicate cancer likelihood greater than 50% based on the discriminant score obtained within each ROI. The bottom right panel shows the co-registered histology with metastatic regions demarcated in green by the pathologist. Figure 2 indicates that the metastatic foci were well detected in the B-mode images augmented with cancer likelihood.

Figure 2 also reveals how QUS methods could be incorporated into a desktop-type machine in a pathology laboratory and permit the efficient guidance of the pathologist towards suspicious regions in the lymph nodes. Such a pathology tool could help drastically reduce the current rate of false-negative determinations when assessing lymph-node status using current standards of care.

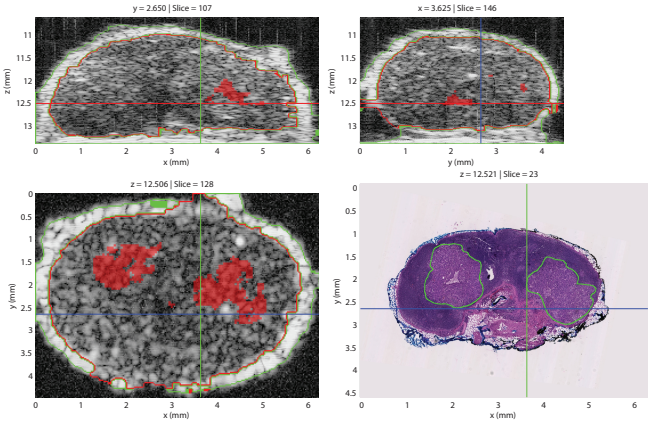

Figure 2: (Cross-sectional parametric images of a partially metastatic lymph node from a breast-cancer patient. Red highlights symbolizes cancer likelihood greater than 50%. Co-registered histology photo micrograph showing metastatic regions in green is also shown.

4 Conclusions

The results obtained in this study demonstrate that 3D QUS methods at high frequencies can detect metastases in dissected lymph nodes with satisfactory sensitivity and specificity. Therefore, the results to date suggest that these methods have great potential for the specific detection and localization of micrometastases often missed during conventional histology. These studies could serve as a basis for the development of a low-cost and small footprint pathology tool to quickly guide pathologist towards suspicious regions using QUS-based methods. Such a tool could be invaluable to reduce the current rate of false-negative determinations.

Acknowledgments

This research was supported by NIH Grant CA100183, the Riverside Research Fund for Biomedical Engineering Research, and CNRS.

References

[1] E. J. Feleppa, J. Mamou, C. R. Porter, and J. Machi, "Quantitative ultrasound in cancer imaging," *Semin Oncol*, vol. 38, no. 1, pp. 136–50, 2011.

[2] R. M. Vlad, S. Brand, A. Giles, M. C. Kolios, and G. J. Czarnota, "Quantitative ultrasound characterization of responses to radiotherapy in cancer mouse models," *Clin Cancer Res*, vol. 15, no. 6, pp. 2067–75, 2009.

[3] F. L. Lizzi, M. Greenebaum, E. J. Feleppa, M. Elbaum, and D. J. Coleman, "Theoretical framework for spectrum analysis in ultrasonic tissue characterization," *J. Acoust. Soc. Am.*, vol. 73, pp. 1366–1373, April 1983.

[4] J. Mamou, M. L. Oelze, W. D. O'Brien, Jr., and J. F. Zachary, "Extended three-dimensional impedance map methods for identifying ultrasonic scattering sites," *J Acoust Soc Am*, vol. 123, pp. 1195–1208, 2008.

[5] J. Mamou, O. Aristizabal, R. H. Silverman, J. A. Ketterling, and D. H. Turnbull, "High-frequency chirp ultrasound imaging with an annular array for ophthalmologic and small-animal imaging," *Ultrasound Med Biol*, vol. 35, no. 7, pp. 1198–208, 2009.

[6] R. H. Silverman, J. A. Ketterling, J. Mamou, and D. J. Coleman, "Improved high-resolution ultrasonic imaging of the eye," *Arch Ophthalmol.*, vol. 126, pp. 94–97, 2008.

[7] J. Mamou, A. Coron, M. Hata, J. Machi, E. Yanagihara, P. Laugier, and E. J. Feleppa, "Three-dimensional high-frequency characterization of cancerous lymph nodes," *Ultrasound Med Biol*, vol. 36, pp. 361–375, 2010.

[8] J. Mamou, A. Coron, M. L. Oelze, E. Saegusa-Beecroft, M. Hata, P. Lee, J. Machi, E. Yanagihara, P. Laugier, and E. J. Feleppa, "Three-dimensional high-frequency backscatter and envelope quantification of cancerous human lymph nodes," *Ultrasound Med Biol*, vol. 37, no. 3, pp. 345–57, 2011.

[9] M. F. Insana, R. F. Wagner, D. G. Brown, and T. J. Hall, "Describing small-scale structure in random media using pulse-echo ultrasound," *J. Acoust. Soc. Am.*, vol. 87, pp. 179–192, 1990.

[10] R. F. Wagner, M. F. Insana, and D. G. Brown, "Statistical properties of radio-frequency and envelope-detected signals with applications to medical ultrasound," *J Opt Soc Am A*, vol. 4, no. 5, pp. 910–922, 1987.

[11] T. Yamaguchi and H. Hachiya, "Proposal of a parametric imaging method for quantitative diagnosis of liver fibrosis," *J Med Ultrasonics*, vol. 37, pp. 155–166, 2010.